Revisiting the brain anatomy of the early Oligocene eutherian mammal *Leptictis* based on virtual endocasts

CARL C. VAN GENT, JOHN R. WIBLE, STEPHEN L. BRUSATTE, LAWIZA KAMRAN, and ORNELLA C. BERTRAND

Van Gent, C.C., Wible, J.R., Brusatte, S.L., Kamran, L., Bertrand, O.C. 2026. Revisiting the brain anatomy of the early Oligocene eutherian mammal *Leptictis* based on virtual endocasts. *Acta Palaeontologica Polonica* 71 (3): 519–534.

Leptictidae are an extinct early Cenozoic group of mammals that has been challenging to place phylogenetically within Eutheria. They have been considered closely related to various crown placental groups such as Lipotyphla, Macroscelidea, or Euarchontoglires based on their "insectivore-grade" features, or as very early placentals or even non-placental eutherians because of their plesiomorphies. Since the 1920s their brain anatomy has been studied using natural endocasts, and oftentimes they are viewed as a model for the ancestral neurosensory conditions of placentals. Here, we use computed tomography (CT) for the first time to generate digital endocranial casts of two species of the canonical early Oligocene leptictid genus, *Leptictis*. Both species present similar endocranial anatomies with variation in the number of condyloid canals and the enclosure of the inferior petrosal sinus. Critically, we find differences compared to descriptions of natural endocasts, most notably that the rhinal fissure is more dorsally positioned, suggesting that *Leptictis* did not have a particularly expanded neocortex compared to Lipotyphla, Afrosoricida, and Macroscelidea. Furthermore, *Leptictis* was not particularly encephalized, and its brain size relative to body size was within the range of modern insectivorous taxa and Eocene mammals generally. Similar endocranial features in *Leptictis* and *Eoryctes* are likely plesiomorphic and do not represent a close phylogenetic relationship, and brain anatomy does not clarify the troublesome relationships of leptictids. The small neocortex and petrosal lobules might reflect fossorial adaptations in *Leptictis*, but more endocranial data from other Leptictidae will be fundamental to better understand any neurosensory shift that may have occurred within this group.

Key words: Mammalia, Eutheria, Leptictidae, endocranial anatomy, neocortex, olfactory bulbs, petrosal lobules, inferior colliculi, Orellan, Oligocene.

Carl C. van Gent [carl.v.gent@gmail.com; ORCID: https://orcid.org/0009-0001-8609-5922], School of GeoSciences, University of Edinburgh, Grant Institute, Edinburgh, Scotland, EH8 9XP, UK.

John R. Wible [WibleJ@CarnegieMNH.Org; ORCID: https://orcid.org/0000-0002-0721-1228], Section of Mammals, Carnegie Museum of Natural History, Pittsburgh, 15206 PA, USA.

Stephen L. Brusatte [stephen.brusatte@ed.ac.uk; ORCID: https://orcid.org/0000-0001-7525-7319], School of GeoSciences, University of Edinburgh, Grant Institute, Edinburgh, Scotland, EH8 9XP, UK; Section of Mammals, Carnegie Museum of Natural History, Pittsburgh, 15206 PA, USA; New Mexico Museum of Natural History and Science, Albuquerque, 87104 NM, USA.

Lawiza Kamran [lawizak23@gmail.com; ORCID: https://orcid.org/0009-0008-8740-3772], School of Biosciences, University of Sheffield, Sheffield S10 2TN, UK

Ornella C. Bertrand [ornella.bertrand@icp.cat; ORCID: https://orcid.org/0000-0003-3461-3908] (corresponding author), School of GeoSciences, University of Edinburgh, Grant Institute, Edinburgh, Scotland, EH8 9XP, UK; Institut Català de Paleontologia Miquel Crusafont, Universitat Autònoma de Barcelona, Edifici ICTA-ICP, c/ Columnes s/n, Campus de la UAB, 08193 Cerdanyola del Vallès (Barcelona), Spain.

Received 14 February 2026, accepted 6 May 2026, published online 3 September 2026.

Introduction

Leptictidae are a family of extinct mammals that are well represented in the fossil record especially from the Paleocene to the Oligocene (e.g., Novacek 1977; McKenna and Bell 1997; Gunnell et al. 2008). Potentially, they also had latest Cretaceous relatives, which would make them one of the few clades of eutherian mammals known to cross the Cretaceous/Paleogene boundary (Velazco et al. 2022). The taxonomic placement of Leptictidae has been long debated,

and this family has been considered closely related to many different clades of placental mammals, including Lipotyphla, Macroscelidea, and various groups within Euarchontoglires (e.g., Van Valen 1965; Novacek 1986; Rose 1999; Asher et al. 2003; O'Leary et al. 2013). We used the term Lipotyphla instead of Eulipotyphla following Asher and Helgen (2010). In some large-scale phylogenetic analyses, they have also been found outside of the placental crown and therefore considered stem placental mammals—and thus a key outgroup for understanding the origin and ancestral morphologies of placentals (e.g., Wible et al. 2007; Velazco et al. 2022). This incongruence stems, at least in part, from the fact that leptictids display ancestral features of crown placental mammals (Novacek 1982). Leptictidae have been found in Asia (Kellner and McKenna 1996; Tong and Wang 2006) and in North America, where they were most diverse and abundant. Previously, European Leptictida were considered part of the family Leptictidae (McKenna and Bell 1997), but are now considered to be part of another family: Pseudorhynchocyonidae (Morlo et al. 2004; Rose 2012; Hooker 2013).

A total of 13 leptictid genera are currently known from North America, including five from the Paleocene and Paleocene/Eocene boundary (Gidley 1915; Matthew and Granger 1921; Matthew 1929; Van Valen 1967; Gingerich and Smith 2006), and several others from the Eocene and Oligocene (Leidy 1868; Matthew 1899; Novacek 1977; Meehan and Martin 2010, 2012; Velazco and Novacek 2016; Gunnell et al. 2016; Korth 2022).

The early Oligocene taxon *Leptictis*, and specifically the species *Leptictis haydeni* Leidy, 1868, and *Leptictis dakotensis* (Leidy, 1868), have been well known for over 150 years, as they were described for the first time by Leidy (1868). There are currently nine recognized species belonging to *Leptictis* (Gunnell et al. 2008; Korth 2022). *Leptictis haydeni* has been accepted as the type of *Leptictis* even though it was only known from one specimen, a cranium (see Gunnell et al. 2008; Meehan and Martin 2010; Wible and Bertrand 2024). *Leptictis* had morphological features indicating cursorial and potentially saltatorial locomotion, including hind limbs that were relatively long in comparison to its forelimbs (Rose 2006). Other aspects of the forelimb morphology also support digging adaptations (Rose 2006). Additionally, some specimens of *Leptictis* have been found in fossilized burrows from the early Oligocene (Sundell 1997). Previous work suggested that *Leptictis* may have eaten preferentially small vertebrates based on its broad snout; another leptictid, *Blacktops* has a narrower snout and was thought to have a diet including invertebrates such as arthropods and worms (Meehan and Martin 2012). Based on the dentition, it is likely that *Leptictis* was to some degree insectivorous and omnivorous (Gunnell and Bloch 2008).

Leptictis has been central to discussions of mammal brain evolution for over a century. The first description of the brain endocast of *Leptictis* was made by Moodie in 1922, based on a physical sediment infill cast of the endocranial cavity. Later, Novacek (1982, 1986) published a more detailed description, also using physical casts, that critiqued the results from Moodie (1922) (e.g., position of the rhinal fissure). Moodie (1922) examined three different specimens that he identified as *Ictops* (now recognized as *Leptictis*; see Novacek 1976). These specimens were attributed to *Leptictis acutidens*, but without certainty because of the lack of associated osteological elements (Moodie 1922). Novacek (1982, 1986) studied more than 30 specimens of *Leptictis dakotensis* from different museum collections with various degrees of preservation that allowed the observation of the brain endocast. *Leptictis* was viewed as having a derived brain morphology based on the observation that the neocortex was relatively well developed (Novacek 1982, 1986). Novacek (1982) made the majority of his comparisons with three clades: Macroscelidea (Afrotheria), Afrosoricida (Afrotheria), and Lipotyphla (Laurasiatheria) that were once classified in the now invalid order "Insectivora", but currently are known to be distributed across the placental mammal family tree (Seiffert 2007; Murphy et al. 2021).

Here, we provide a new look at the brain of *Leptictis* based for the first time on digital endocasts generated from high-resolution computed tomography (CT) scanning. We describe the endocranial anatomy of two *Leptictis* specimens belonging to two different species from the Brule Formation in South Dakota (Oligocene, Orellan North American Land Mammal Age). The virtual endocast of the brain of *L. haydeni* (ANSP 11402), the type of the genus *Leptictis*, is described here for the first time and compared to data from *L. dakotensis* (SDSM 62369). Past studies used natural brain endocasts, which might limit the amount of information that can be extracted, as natural endocasts are often incomplete, whereas our CT data allow us to construct high-resolution 3D models of the brain endocasts. Therefore, we revisit the hypotheses made by Novacek (1982) about the brain of *Leptictis* including its morphology (e.g., presence of sulci, exposure of the midbrain), its relative size, and the size of its components (i.e., neocortex and the olfactory bulbs). Through the digital reconstruction of the brain of the two *Leptictis* specimens, we aim to shed some light on the ecology and behavior of *Leptictis* and its phylogenetic relationships with other mammals.

Institutional abbreviations.—AMNH F: AM, Frick collection: American Museum of Natural History, New York, USA; ANSP, Academy of Natural Sciences, Philadelphia, USA; UM, Museum of Paleontology, University of Michigan, Ann Arbor, USA; SDSM, South Dakota School of Mines Museum, Rapid City, USA.

Other abbreviations.—CRMW, cerebrum maximal width; CLMW/L, cerebellum maximal width/length; EQ, encephalization quotient; NALMA, North American land mammal age; OL/W/H, olfactory bulb length/width/height; PEQ, phylogenetic encephalization quotient; TL, total endocast length. We follow standard convention in abbreviating tooth families as I, C, P, and M, with upper and lower case letters referring to upper and lower teeth, respectively.

Material and methods

Specimens under study.—We constructed digital endocasts of two *Leptictis* specimens using CT data. The first of these, a specimen of *Leptictis haydeni* (ANSP 11402), is from Mauvaises Terres in the White River Group of South Dakota (named "Mauvais Terraces" in Janis et al. 2008). This locality is part of the Oligocene Brule Formation and more specifically the Orellan NALMA. ANSP 11402 is the type and only known specimen of *L. haydeni* (Novacek 1976; Wible and Bertrand 2024). The second specimen, initially referred to *Leptictis* sp. (SDSM 62369), is from another locality, Reva Gap, Slim Buttes (Harding County, South Dakota), also from the Orellan of the Brule Formation (Janis et al. 2008). SDSM 62369 is most similar to *Leptictis dakotensis* in terms of its size and craniodental morphology and was therefore referred to *L. dakotensis* in Wible and Bertrand (2024). The Orellan NALMA indicates an age 33.9–32.1 Ma for both specimens (ages from Vandenberghe et al. 2012). *Leptictis haydeni* (ANSP 11402) is well preserved with a complete cranium slightly distorted mediolaterally. *Leptictis dakotensis* (SDSM 62369) also shows little to no signs of crushing, though it is missing the zygomatic arches on both sides of the cranium (Fig. 1). We also had access to two natural endocasts of *Leptictis*: one of *Leptictis* sp. AMNH F: AM 87458 (Chalky Buttes SE, North Dakota; Orellan NALMA; see Wahlert 2004) and one of *L. dakotensis* AMNH F: AM 96730 (see Novacek 1982: fig. 1). The basicranial anatomy and the vascular and nervous systems of ANSP 11402 and SDSM 62369 have recently been described in Wible and Bertrand (2024). In terms of the nomenclature, we follow previous publications to describe the endocranial anatomy of the endocasts (e.g., Silcox et al. 2010; Harrington et al. 2016; Bertrand et al. 2020, 2024; Vincent et al. 2025), nerves and vessels (Wible and Bertrand 2024) of *Leptictis*. One exception corresponds to the use of the term orbitotemporal canal in *Leptictis*, which is technically not fully enclosed in a bony canal when it is lateral to the cerebrum (within the middle cranial fossa) and instead leaves a groove on the endocranial surface (Wible and Bertrand 2024). Therefore, we refer to orbitotemporal vessels instead of canal. We elected to describe the endocasts without comparing them to other mammals because of the very uncertain phylogenetic position of *Leptictis*. In

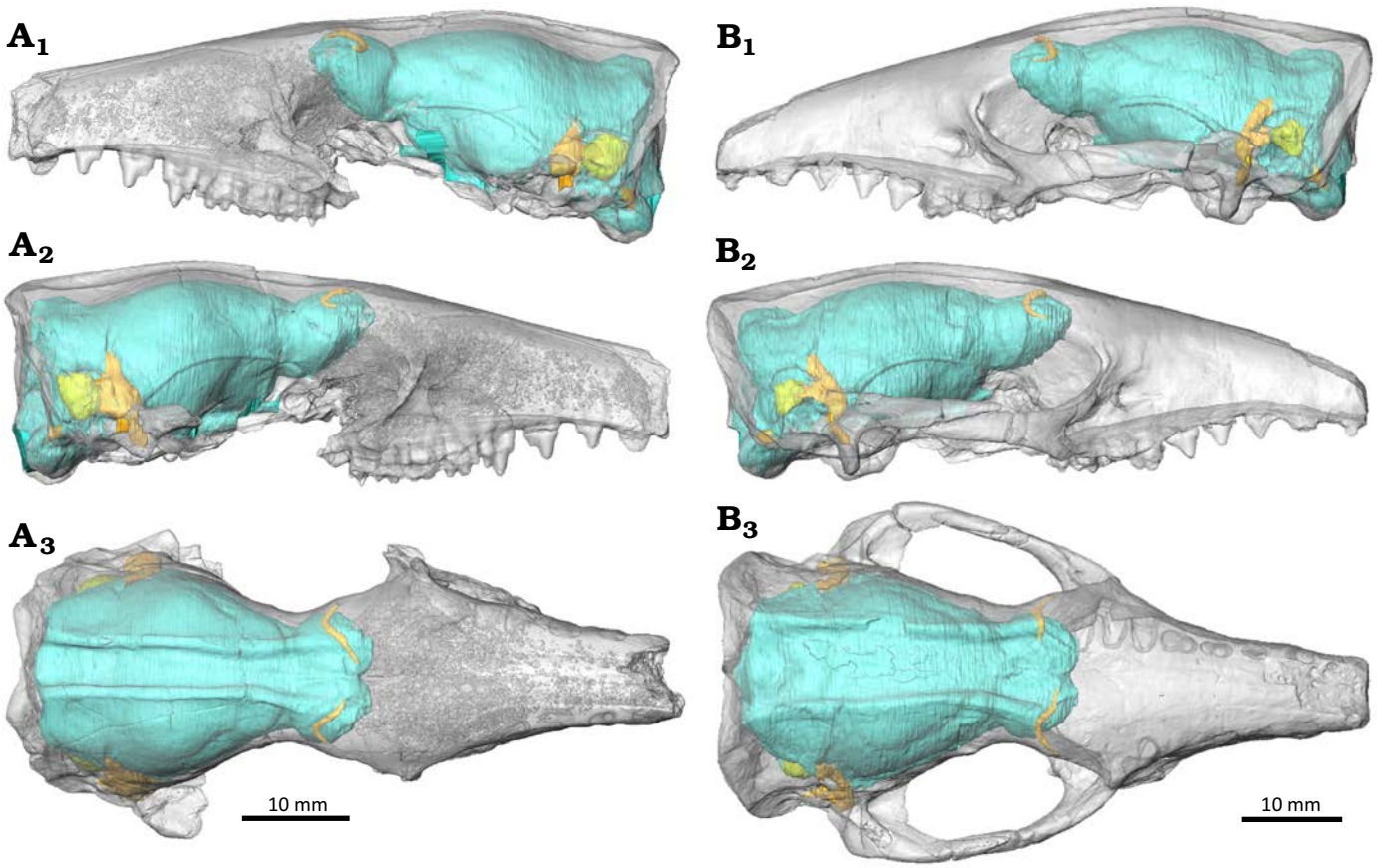

Fig. 1. Translucent renderings crania with their virtual endocasts inside of *Leptictis dakotensis* (Leidy, 1868), SDSM 62369 (**A**) from Orellan, Oligocene, Brule Formation, Reva Gap, Slim Buttes, Harding County, South Dakota, USA and *Leptictis haydeni* Leidy, 1868, ANSP 11402 (**B**) from Orellan, Oligocene, Brule Formation, Mauvaises Terres, White River Group, South Dakota, USA. Left (A_1, B_1) and right (A_2, B_2) lateral and dorsal (A_3, B_3) views. Different colors were used to depict the endocasts that correspond to what is calculated for the brain endocast (blue) and the petrosal lobule (green) volumes in Avizo. The parts in gold correspond to vessels in bony canals that are not included in the endocranial volume in order to not overestimate the volume of the endocranial cavity.

the discussion, we make comparison with other mammals concerning relevant anatomical features such as the rhinal fissure, orbitotemporal vessels, the presylvian sulcus and the orbital gyrus.

Virtual endocast acquisition.—The two specimens were scanned at the Microscopy and Imagery Facility (MIF) at the American Museum of Natural History (AMNH). The scanning parameters for *L. haydeni* (ANSP 11402) were: voltage of 190 kV, current of 180 µA and a voxel size of 0.04348457 mm and for *L. dakotensis* (SDSM 62369), the voltage and current where respectively of 170 kV and 190 µA and the voxel size was of 0.03438626 mm. The two specimens were segmented in AvizoLite® 2020.3 software (Thermo Fisher Scientific). We created new labelfield modules to segment the brain endocasts for both specimens. *Leptictis dakotensis* (SDSM 62369) was segmented by OCB (see Bertrand et al. 2022) and *L. haydeni* (ANSP 11402) by CCvG. We used the Avizo pen tool to draw the boundaries between the fossilized bone and endocranial space because the endocranial cavity was filled with matrix that had a similar density to the bone. In instances where the bone was not preserved, straight lines were traced from the two nearest pieces of bone. Interpolation was performed between approximately three slices. To estimate the volume of the brain endocasts, we generated their surface rendering using unconstrained smoothing in Avizo. The volume of the olfactory bulbs was measured using the "Volume Edit tool" in Avizo. For the petrosal lobules, they were re-segmented, so their volume could be quantified similarly to the endocranial volume. The function "Surface Area Volume" was used to obtain the values of the endocranial, olfactory and petrosal lobule volumes. To measure the neocortical surface area, we used the previously obtained surface of the endocast and isolated the neocortex manually from the rest of the endocast. Then, the function "extract surface" was used to obtain the value for the surface area of the neocortex.

Body mass and encephalization quotient estimations.—For this study, we employed different equations to estimate the body mass of the studied individuals. We used dental, cranial, and postcranial data to determine the body mass of *L. dakotensis* and cranial data only for *L. haydeni*, as the one known specimen consists solely of a cranium. All of the body mass formulas were taken from the literature (Table 1). We used the mammal equation of the m1 of Legendre (1989) and the m1 "non selenodont taxa" equation from Damuth (1990). For the cranial length equation, we used the one created by Bertrand et al. (2022) that was based on a sample of mammals produced by Kirk et al. (2014). Further estimations of body mass were done using postcranial elements, more specifically, the length of the femur and the humerus, using formulas put forth by Campione and Evans (2012). We recognize that the circumference of the femur and the humerus would be better estimators of body mass (as noted by Campione and Evans 2012), but we did not have access to these specimens to make these measurements. The osteological data used to obtain the body mass for *L. dakotensis* were from different specimens (Table 2). For the m1, we use the data published by Meehan and Martin (2010), and the lengths of the humerus and femur are from Rose (2006). We note that the estimation of the cranial length of *L. dakotensis* (SDSM 62369) is slightly underestimated as the tip of the nasal is broken. For *L. haydeni* (ANSP 11402), we used the cranial

Table 1. Equations used to calculate the body masses (measurements in mm) of both specimens of *Leptictis*. Abbreviations: BM, body mass; CL, cranial length; FL, femur length; HL, humerus length; LN, natural logarithm; LOG10, logarithm with base 10; OCW, occipital condylar width.

Equation	Formula	References
Dental	10^(3.17 × (LOG10(m1 length)) + 1.04)	Damuth 1990: non selenodont taxa
	10^(1.51 × (LOG10(m1 area)) + 1.44)	Damuth 1990: non selenodont taxa
	EXP(1.7054 × (LN(m1 area)) + 2.247)	Legendre 1989: mammals
Cranial	10^(3.4082*(LOG10(CL)) - 3.3039)	Bertrand et al. 2022; sample from Kirk et al. 2014
Occipital condyle	EXP(7.70727*(LN(OCW)^(2/3))) - 8.21527	Engelman 2022: therians only
Postcranial	2.993*(LOG10(FL)) - 2.341	Campione and Evans 2012: femur length
	2.8626*(LOG10(HL)) - 1.8476	Campione and Evans 2012: humerus length

Table 2. Osteological measurements (in mm) used to determine the body mass of both specimens of *Leptictis*. * slightly underestimated (broken tip of the nasal).

Measurements	Source	*Leptictis dakotensis*		*Leptictis haydeni* (ANSP 11042)
m1 length	Meehan and Martin 2010	AMNH 38915	3.14	–
m1 width			4.37	–
m1 area width/length ratio			13.72	–
cranial length	this study	SDSM 62369	62.575*	65.78
occipital condylar width	this study		–	16.24
femur length	Rose 2006	JPC-002	54	–
humerus length			36.7	–

length and the occipital condylar width (Engelman 2022) to estimate its body mass (Table 2). Because of deformation to *L. dakotensis* (SDSM 62369), we were not able to obtain an accurate measure of the occipital condylar width. The body masses for both specimens are relatively close. An average value of 742.95 g was obtained for *L. dakotensis* and of 966.89 g for *L. haydeni* (Table 3).

We calculated the encephalization quotient (EQ) based on the equations from Jerison (1973) and Eisenberg (1981) to allow comparisons of relative brain size with previously published mammal specimens and the results obtain for *Leptictis* by Novacek (1982). The PEQ (phylogenetic encephalization quotient) was also calculated for future reference using the equation for all mammals from Burger et al. (2019) and are presented in SOM: table S1 (Supplementary Online Material available at http://app.pan.pl/SOM/app71-VanGent_etal_SOM.pdf. The EQ corresponds to the ratio of the actual brain size (E_i) of a species "i" and the expected brain size for a hypothetical mammal of similar body mass (E_c) Martin (1990). The following equations were used: EQ = brain size/(0.12*(body mass)^0.67, Jerison (1973) and EQ = brain size/(0.0553*(body mass)^0.74, Eisenberg (1981). We used both equations because the samples used to make these equations led to EQs being underestimated with Jerison (1973)'s equation and overestimated with the one from Eisenberg (1981) (see Bertrand et al. 2019).

Neurobiological measurements.—We produced ratios of the olfactory bulb and petrosal lobule volumes and neocortical surface area in relation to both endocranial size and body mass (Table 4). Linear measurements were taken on the virtual endocasts of both specimens and ratios were calculated based on Bertrand and Silcox (2016), but they have also been applied to other mammals (Bertrand et al. 2024; Cabasés Bru et al. in press). Ratios of these linear measurements were produced (Table 4). In the discussion, we also quantitatively compare the brain endocast of *Leptictis* with Macroscelidea, Afrosoricida, and Lipotyphla using boxplots of the EQ, neocortical and olfactory bulb percentage ratios (%) to revisit previous conclusions from Novacek (1982) about the senses of *Leptictis*. To make these boxplots, we used data from different sources (Stephan et al. 1991; Boddy et al. 2012; Benoit et al. 2013). For one particular specimen of the dataset (*Galegeeska revoilii*), its body mass was obtained from Smith et al. (2003). For the EQ boxplot, the endocranial volumes of both specimens of *Leptictis* and of the data from Benoit et al. (2013) were converted to brain mass using the equation from Stephan et al. (1981) to be comparable to the rest of the data. The neocortical and olfactory volumes were converted to neocortical and olfactory bulb masses in order to produce ratios of these two structures vs. brain mass. For *Leptictis* and the data from Benoit et al. (2013), we used the surface of the endocasts and of the neocortex to produce neocortical ratios. The boxplots were generated using the R packages "ggplot2" (Wickham 2016) in R studio (R v4.5.2; R Core Team 2019).

Table 3. Body mass estimations (in g) of both specimens of *Leptictis*.

Body mass estimations based on	*L. dakotensis* (SDSM 62369)	*L. haydeni* (ANSP 11402)
m1 area, equation Legendre 1989	823.38	–
m1 length	412.35	–
m1 area, equation Damuth 1990	1437.11	–
cranial length	658.56	780.78
occipital condylar width	–	1153.01
femur length	698.32	–
humerus length	427.97	–
Average body mass	742.95	966.89

Table 4. Linear measurements, surface areas, volumes, EQ, body mass measurements and their ratios for the specimens of both studied species of *Leptictis*. The values in bold are published in Bertrand et al. (2022). CLMW/L, cerebellum maximal width/length; CRML/W/H, cerebrum maximal length/width/height; OL/W/H; olfactory bulb length/width/height; TL, total endocast length; T/NS, total endocast/neocortical surface area; T/O/PV, total endocast/olfactory bulb/petrosal lobule volume.

	Leptictis dakotensis (SDSM 62369)	*Leptictis haydeni* (ANSP 11402)
Linear measurements (mm)		
TL	31.67	33.80
OL	7.44	7.86
OW	12.28	12.93
OH	7.6	8.02
CRML	16.71	17.43
CRMW	18.72	20.38
CRMH	13.54	13.34
CLML	7.85	8.76
CLMW	17.96	19.31
Ratios linear measurements (%)		
OL/TL	23.49	23.25
OL/OW	60.59	60.79
OL/OH	97.89	98.00
CRML/TL	52.76	51.57
CLMW/CRMW	95.94	94.75
OW/CRMW	65.60	63.44
OW/CLMW	68.37	66.96
OL/CRMH	54.95	58.92
Surface areas and volumes		
TS (mm^2)	2034.72	2192.61
NS (mm^2)	268.79	246.84
TV (mm^3)	4307.64	5114.89
OV (mm^3)	406.38	429.86
PV (mm^3)	70.40	32.80
Ratios surface areas and volumes (%)		
OV/TV	9.43	8.40
OV/BM	0.05	0.04
PV/TV	1.63	0.64
PV/BM	0.009	0.003
NS/TS	13.21	11.26
NS/BM	0.04	0.03
Encephalization Quotient (EQ)		
EQ: Jerison 1973	0.43	0.43
EQ: Eisenberg 1981	0.58	0.57
Body mass (g)	742.95	966.89

Results

Overall brain endocast and encephalization quotient.—Both crania are well preserved and there is no noticeable deformation that may affect the measurements of volumes, surfaces, and linear dimensions. The virtual brain endocasts of *L. dakotensis* (SDSM 62369) and *L. haydeni* (ANSP 11402) differ moderately in absolute size but show broadly similar proportional relationships among major brain regions. In terms of ratios of the linear measurements, both specimens have overall very similar proportions including the ratio of the total endocast length and maximal width of the cerebrum representing the maximum width of the endocast (TL/CRMW; Table 4). Based on both virtual endocasts, the total endocranial volume (TV) is about 4–5 cm^3 (Table 4), which corresponds to a brain that would potentially exhibit sulci and be gyrencephalic based on previous studies (e.g., Bauchot and Stephan 1967; Striedter 2005; Macrini et al. 2007). From the estimated body masses (Table 4) obtained using osteological proxies, the encephalization quotient calculated following Jerison (1973) is 0.43 for both specimens. Using Eisenberg's (1981) equation, EQ values are higher and correspond to 0.58 for *L. dakotensis* and 0.57 for *L. haydeni* (Table 4).

Olfactory bulbs.—The olfactory bulbs of *L. haydeni* and *L. dakotensis* are positioned dorsal to the anterior aspect of the M3 (Fig. $1A_1$, B_1). Both specimens have very similarly shaped olfactory bulbs, although they are proportionally slightly more anteroposteriorly elongated in *L. dakotensis* compared to the rest of the endocast (Fig. $2A_1$; Table 4: OL/TL). In dorsal view, the olfactory bulbs are elliptical in shape, and they are mediolaterally wider in the posterior compared to the anterior aspect (Fig. 2A). The olfactory bulbs are antero-posteriorly conjoined on the midline in both specimens, and there is no bone that separates them (Fig. 2A). The cast of the superior olfactory sinus is positioned medial to each olfactory bulb and is visible in dorsal view on both specimens (Fig. 2A). In lateral view, the olfactory bulbs are triangular in overall shape, and the upper posterior margin of the olfactory bulb is convex while the lower posterior margin is more concave (Fig. $3A_1$, B_1).

In terms of proportions and size, the olfactory bulbs are similarly developed in both *Leptictis* species with equivalent ratios of the olfactory bulb length vs. olfactory bulb width and height (OL/OW and OL/OH; Table 4). The olfactory bulbs are nearly as tall as they are long in both taxa, with OL/OH ratios of 97.89% (*L. dakotensis*) and 98.00% (*L. haydeni*; Table 4). The olfactory bulbs correspond to 9.43% of the endocranial volume in *L. dakotensis* and a slightly smaller proportion of 8.41% in *L. haydeni* (see Fig. 4C using data from SOM: table S1). Relative to estimated body mass, olfactory bulb volume represents a similar proportion in *L. dakotensis* (0.05%) and in *L. haydeni* (0.06%; Table 4).

Cerebrum and midbrain.—The virtual endocasts of *L. haydeni* and *L. dakotensis* display a circular fissure separating the olfactory bulbs from the cerebrum (Figs. 2, 3). The olfactory bulbs and the circular fissure are not covered by the cerebrum anteriorly (Fig. 2A), indicating that the frontal lobes of the cerebrum were not expanded in contrast to many modern mammals such as in primates, elephants, and whales (Herculano-Houzel 2012: fig. 1). The cerebrum is composed of two main regions: the neocortex and the paleocortex, which are separated by the rhinal fissure (Martin 1990). This feature is an important landmark that has been used to determine the degree of development of the neocortex in mammals (Jerison 2012; Long et al. 2015). In some mammalian groups, the rhinal fissure and the orbitotemporal vessels overlap (i.e., Euarchontoglires; e.g., Silcox et al. 2010; Bertrand et al. 2017). However, some mammals show a different configuration wherein the rhinal fissure is located dorsal to the orbitotemporal vessels (e.g., Orliac et al. 2012; Benoit et al. 2013; Cabasés Bru et al. in press), which is related to the neocortex being less expanded than in taxa in which the rhinal fissure and the orbitotemporal vessels overlap. Both studied specimens of *Leptictis* show the first condition in which the rhinal fissure is located dorsal to the orbitotemporal vessels (Figs. 2A, $3A_2$, B_2).

The position of the orbitotemporal vessels as ventral to the rhinal fissure is more clearly observable in the lateral view of *L. haydeni* than in *L. dakotensis* (Fig. $3A_1$, B_1). In dorsal view, the rhinal fissure is well demarcated in both specimens (Fig. 2A). In lateral view, the rhinal fissure is directed anterodorsally, while the orbitotemporal vessels are anteriorly to slightly anteroventrally oriented (Fig. 3). All of the boundaries of the neocortex are visible in dorsal view, suggesting a limited expansion of this structure (Fig. 2A). In the same view, the overall shape of the cerebrum of both specimens is triangular with the anterior aspect of the cerebrum being narrower mediolaterally than the posterior region (Fig. 2A). In ventral view, the olfactory peduncles are more distinguishable from the rest of the paleocortex in *L. dakotensis* compared to *L. haydeni* (Fig. 2B).

The midbrain is visible, but the colliculi of the midbrain are not preserved on the surface on either virtual endocast. The midbrain is not covered by the cerebellum posteriorly or by cerebrum anteriorly (Fig. 2A), which might suggest that the colliculi might be covered by other tissues. However, the inferior colliculi are visible on the natural endocast of *L. dakotensis* (AMNH F: AM 87458; Fig. 5A), suggesting intraspecific variation in the visibility of this anatomical feature. The cast of the pituitary gland corresponds to the hypophyseal fossa. This feature is visible in ventral view and is more clearly demarcated in *L. dakotensis* compared to *L. haydeni*, in which the hypophyseal fossa is not visible on the endocranial surface (Fig. 2B). The cerebrum of *L. dakotensis* and *L. haydeni* occupies just over half of the total endocast length, with CRML/TL (cerebrum maximal length vs. total endocast length) ratios of 52.76% and 51.57%, respectively (Table 4).

The neocortex represents a relatively small proportion of the total endocranial surface in both taxa. In *L. dakotensis*, the neocortical surface area accounting for 13.21% of the

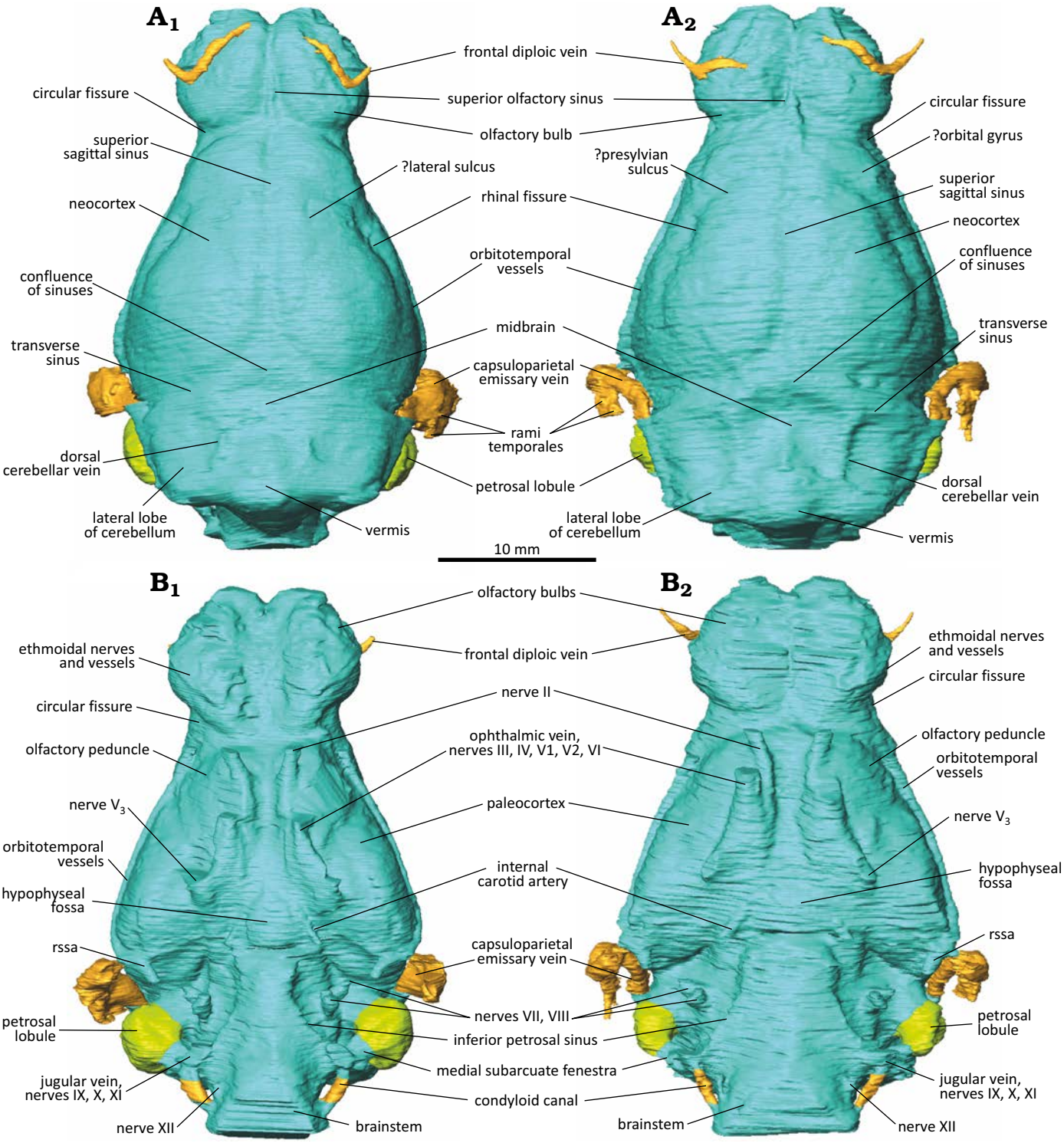

Fig. 2. Virtual reconstructions in dorsal and ventral views of the brain endocasts of *Leptictis dakotensis* (Leidy, 1868), SDSM 62369 (**A**) from Orellan, Oligocene, Brule Formation, Reva Gap, Slim Buttes, Harding County, South Dakota and *Leptictis haydeni* Leidy, 1868, ANSP 11402 (**B**) from Orellan, Oligocene, Brule Formation, Mauvaises Terres, White River Group, South Dakota, USA. In dorsal (A_1, B_1) and ventral (A_2, B_2) views. Abbreviation: rssa, ramus superior of the stapedial artery. Bony canals are in gold, petrosal lobules are in green, the rest of the endocast is in turquoise.

total endocast surface area, whereas in *L. haydeni* it represents a smaller proportion of 11.29% of the total surface area (Table 4; see Fig. 4B using data from SOM: table S1). These values indicate a limited neocortical expansion relative to overall brain size in both species. When compared to body mass, the neocortex also represents a similar proportion in *L. dakotensis* (0.04%) and in *L. haydeni* (0.03%). A lateral sulcus may be present on the endocast of *L. dakotensis* (SDSM 62369), although its identification remains uncertain due to limited clarity of its expression. We also

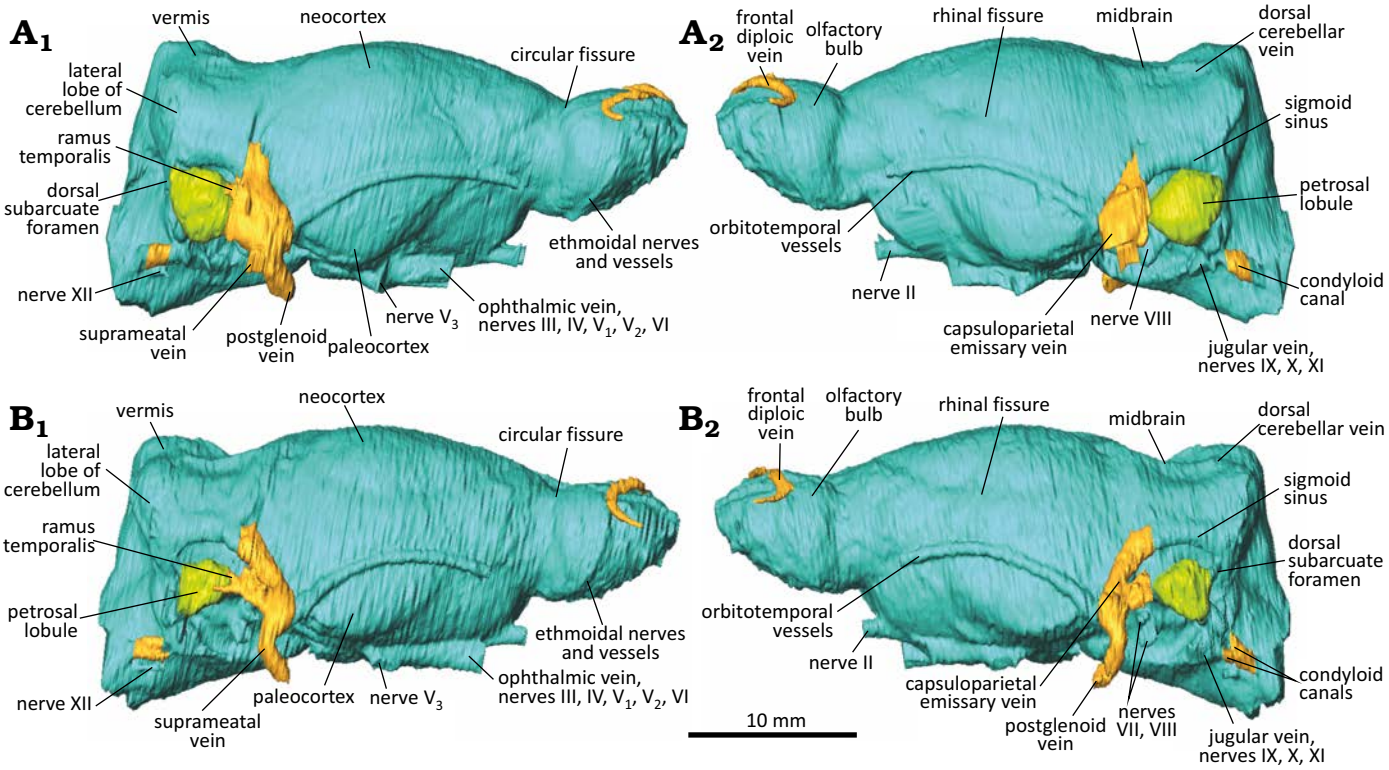

Fig. 3. Virtual reconstructions in lateral views of the brain endocasts of *Leptictis dakotensis* (Leidy, 1868), SDSM 62369 (**A**) from Orellan, Oligocene, Brule Formation, Reva Gap, Slim Buttes, Harding County, South Dakota and *Leptictis haydeni* Leidy, 1868, ANSP 11402 (**B**) from Orellan, Oligocene, Brule Formation, Mauvaises Terres, White River Group, South Dakota, USA. In right (A_1, B_1) and left (A_2, B_2) lateral views. Scale bars 10 mm. Bony canals are in gold, petrosal lobules are in green, the rest of the endocast is in turquoise.

note its presence on the natural endocast of *L. dakotensis* (AMNH F: AM 87458; Fig. 5A). There is also the possible presence of a presylvian sulcus and of the orbital gyrus, which are visible in *L. haydeni* (Fig. $2A_2$) as well as in the two natural endocasts of *L. dakotensis* (AMNH F: AM 87458; Fig. 5A) and *Leptictis* sp. (AMNH F: AM 96730; Fig. 5B). These morphological differences on the endocasts are likely related to preservation and the genus *Leptictis* likely had a lateral and presylvian sulcus (and associated orbital gyrus).

Cerebellum.—In dorsal view, the cerebrum does not overlap onto the cerebellum, leaving the dorsal surface of the cerebellum entirely exposed (Fig. 2A). The lateral lobes of the cerebellum are easily distinguished from the vermis, especially in *L. haydeni*, where the paramedian fissures are well defined on the endocast (Fig. 2A). The petrosal lobules, which fill the subarcuate fossa (Bertrand et al. 2020; Lang et al. 2022), are positioned at the same level as the anterior region of the vermis in dorsal view (Fig. 2A). In lateral view, they are positioned just ventral to a large sigmoid sinus (Fig. $3A_2$, B_2). The petrosal lobules have a more bulbous shape in *L. dakotensis* (Fig. 3A) than in *L. haydeni* (Fig. 3B). In lateral view, the vermis is slightly more ventral than the cerebrum in *L. haydeni*, but they are approximately at the same level in *L. dakotensis* (Fig. 3). In dorsal view, the transverse sinus is visible at the posterior margin of the cerebrum and along the anterior region of the lateral lobe of the cerebellum (Fig. 2A), consistent with its role in draining the posterior cerebral venous system. The transverse sinus and the confluence of sinuses are also visible in the natural endocast of *L. dakotensis* (AMNH F: AM 87458; Fig. 5A).

The cerebellum of *L. dakotensis* and *L. haydeni* shows similar proportions despite differences in absolute size. The cerebellum is nearly as wide as the cerebrum, with CLMW/CRMW (cerebellum maximal width vs. cerebrum maximal width) ratios of 95.94% in *L. dakotensis* and 94.75% in *L. haydeni* (Table 4). The petrosal lobules correspond to 1.63% of total endocast volume and 0.009% of estimated body mass in *L. dakotensis*, while in *L. haydeni*, they represent a smaller percentage of 0.64% of total endocast volume and 0.004% of body mass. These differences indicate potential intraspecific variation in the relative development of the petrosal lobules within the genus *Leptictis*.

Cranial nerves and blood vessels.—Various cranial nerve openings are also visible on the ventral surfaces of both virtual endocasts (Fig. 2B). The ethmoidal nerves and vessels are visible in lateral view on the ventral surface of the olfactory bulbs and exit the cranium through a single foramen in both specimens (Figs. 2B, $3A_1$, B_1). The casts of the optic canal for cranial nerve II (optic) are visible on both virtual endocasts and are located posterior to the olfactory bulbs. However, the optic chiasm does not leave a trace on the surface of the endocast. From the endocast, it can be deduced that both specimens of *Leptictis* lack a foramen

rotundum and therefore the ophthalmic veins and cranial nerves III (oculomotor), IV (trochlear), V_1 (ophthalmic), V_2 (maxillary), and VI (abducens) would have passed through the sphenorbital fissure in *L. haydeni* and *L. dakotensis* (Fig. 2B). This points to a condition that is considered ancestral in placental mammals: the sphenorbital fissure and the foramen rotundum are fused together and therefore cranial nerve V_2 passes through the same opening as nerves III, IV, V_1 and VI (Figs. 2, 3; O'Leary et al. 2013). The cast of cranial nerve V_3 (mandibular) is positioned posterolateral to the sphenorbital fissure. The mandibular nerve V_3 exited via the foramen ovale (Fig. 2B).

Nerves VII (facial) and VIII (vestibulocochlear) exited the endocranial cavity through the internal acoustic meatus—the cast of which is visible on both presently studied specimens (Fig. 2B). In lateral view, those nerves are located ventral to the anterior part of the petrosal lobules (Fig. $3A_2$, B_2). The cast of the jugular foramen is visible on both endocasts and is located posterior to nerves VII and VIII in ventral view (Fig. 2B) and ventral to the posterior end of the petrosal lobules in lateral view (Fig. $3A_2$, B_2). Cranial nerves IX (glossopharyngeal), X (vagus), and XI (accessory) passed through this foramen, as well as the internal jugular vein (Fig. $3A_2$, B_2). Finally, positioned posteriorly to the jugular foramen, the casts of the hypoglossal foramen—which would have housed cranial nerve XII (hypoglossal)—is visible on both endocasts, though it is subject to varying degrees of visibility, likely due to preservation (Figs. 2B; $3A_1$, B_1).

In terms of the venous systems, the superior olfactory sinus is continuous with the superior sagittal sinus, which are visible on the dorsal surface of the virtual endocasts of both specimens (Fig. 2A). The superior sagittal sinus is continuous with the confluence of sinuses, which connects to the transverse sinus—a condition that is considered typical for therian mammals (Fig. 2A; Wible and Rougier 2000). The superior sagittal sinus ran between both hemispheres, being slightly buried within the meninges, a condition seen in other mammals (Macrini et al. 2007). We observed a dorsal cerebellar vein oriented anteroposteriorly that connects to the transverse sinus in both specimens, although it is more visible in *L. haydeni* compared to *L. dakotensis* (Fig. 2A).

The transverse sinus typically gives rise to three branches in placental mammals: the capsuloparietal emissary vein, the sigmoid sinus, and the superior petrosal sinus (e.g., Wible 1984; Novacek 1986; Muizon de et al. 2015). In *Leptictis*, two foramina are associated with the capsuloparietal emissary vein: the postglenoid foramen for the postglenoid vein and the suprameatal foramen for the suprameatal vein (Fig. $3A_1$, B_1; Wible and Bertrand 2024: fig. 7). The sigmoid sinus exited the cranium through the jugular foramen as the internal jugular vein (Fig. $3A_1$, B_1). The sigmoid sinus abuts the cast of the cerebellum laterally and is first directed anteroposteriorly and then ventrally, reaching the jugular foramen posteriorly (Fig. $3A_1$, B_1). The sigmoid sinus is also connected to the condyloid vein via two canals in *L. haydeni* (Fig. $3B_2$) and one canal in *L. dakotensis* (Fig. $3A_2$). The content of the condyloid

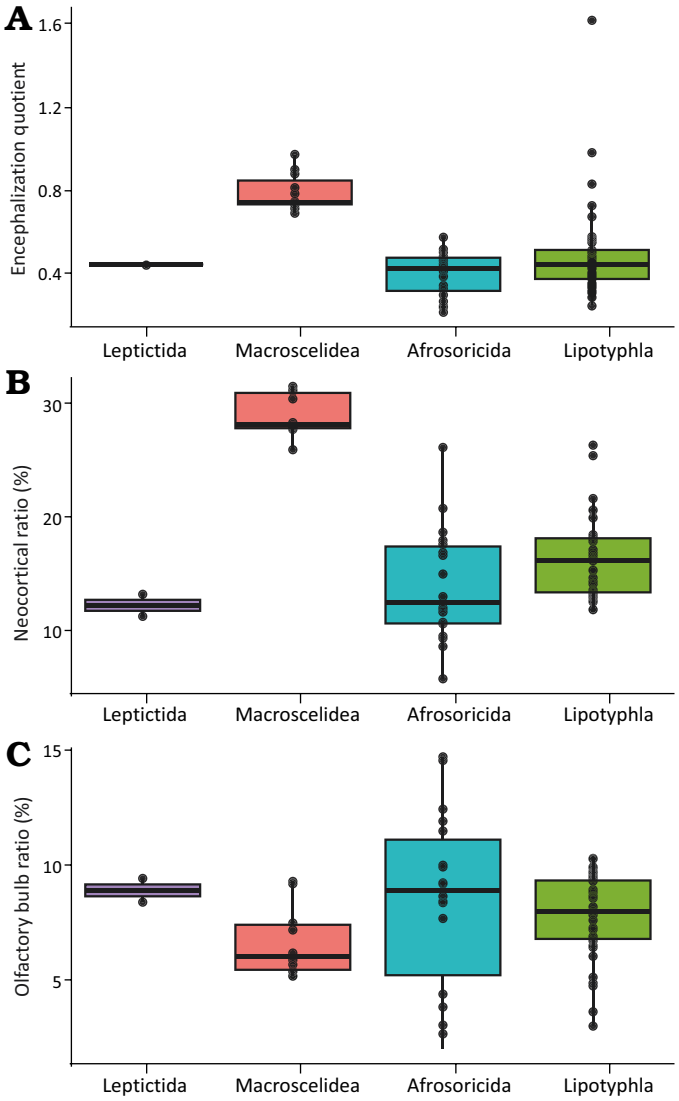

Fig. 4. Boxplots comparing the relative size of the brain and of brain regions of *Leptictis* with Macroscelidea, Afrosoricida, and Lipotyphla. **A**. Encephalization quotient (equation from Jerison 1973). **B**. Neocortical ratio (%). **C**. Olfactory bulb ratio (%).

canal would have exited through the foramen magnum. The superior petrosal sinus appears to be absent in both specimen of *Leptictis* as observed by Wible and Bertrand (2024).

The inferior petrosal sinus was present in both specimens with some variations in terms of its course from the hypophyseal fossa and its exit through the jugular foramen in *L. dakotensis* but through a separate foramen in *L. haydeni* that was described in detailed by Wible and Bertrand (2024). The course of the inferior petrosal sinus was endocranial in *L. dakotensis* (Fig. $2B_1$) and in a small canal in *L. haydeni*. The canal could not be fully traced in *L. haydeni*, but its approximate position can be labelled (Fig. $2B_2$). Both specimens display two openings emerging from the subarcuate fossa that connect to the sigmoid sinus: the dorsal subarcuate foramen and the medial subarcuate fenestra (Figs. 2B, $3A_1$, B_2; Wible and Bertrand 2024). Both specimens display a frontal diploic vein (Wible and Bertrand 2024), but the

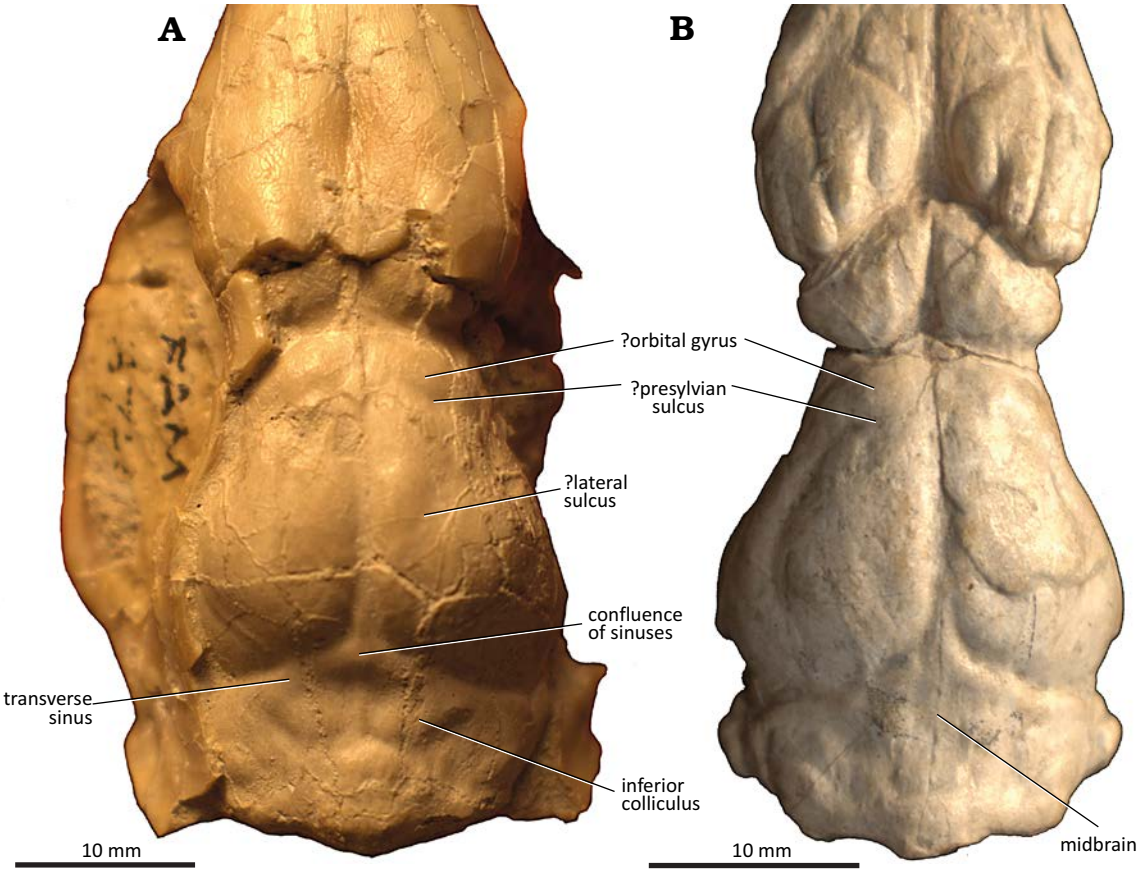

Fig. 5. Natural endocast of the two specimens of the eutherian mammal *Leptictis*. **A**. Endocast still attached to the cranium of *Leptictis dakotensis* (Leidy, 1868) (AMNH F: AM 87458) from Orellan, Oligocene, Chalky Buttes SE, North Dakota, USA. **B**. Natural endocast of *Leptictis* sp. (AMNH F: AM 96730) from an unknown locality.

frontal diploic foramen is located more laterally, further from the olfactory bulbs in dorsal view in *L. haydeni* compared to *L. dakotensis* (Fig. 2A).

Regarding the arterial system, the orbitotemporal vessels correspond to the ramus supraorbitalis, the anterior division of the ramus superior, and accompanying vein (Wible 1987). Rami temporales, which are branches of the posterior division of the ramus superior, and accompanying veins are visible in lateral view in both specimens (Fig. 3A_1, B_1; see also Wible and Bertrand 2024: fig. 7). Finally, the pathway of the internal carotid artery, and of its branch the stapedial artery, was described by Wible and Bertrand (2024). The cast of the stapedial artery was traced in both specimens (Fig. 2B) and has a typical position entering the endocranial cavity on the posterior aspect of the cerebrum in ventral view, similar to other mammals exhibiting the same structure (e.g., Bertrand et al. 2016, 2017).

Discussion

Morphological interpretations of the brain endocasts of *Leptictis*.—Our newly generated digital endocasts, based on CT data, give an updated view of the brain and endocranial anatomy of *Leptictis* using modern techniques. Critically, we can now compare detailed digital endocasts with those in the historical and more recent literature, which were physical structures extracted from the fossils themselves. This reveals similarities and differences, and allows us to provide the most up-to-date view of the brain anatomy of this important early placental (or near-placental) mammal.

Locating the rhinal fissure is the first step in estimating the size of the surface of the neocortex in endocasts. Here, we identify the rhinal fissure as being much more dorsally located than the structure Novacek (1982) identified as the rhinal fissure. In the ~40 years since Novacek's publications, as more endocasts have been produced digitally, we now have a better understanding of the relationship between the rhinal fissure and the orbitotemporal vessels. Novacek (1982) worked with natural endocasts and identified the rhinal fissure as being just ventral to the orbitotemporal vessels. We were not able to see any trace of a fissure in that location in our virtual endocasts. Moodie (1922) also used natural endocasts and identified the rhinal fissure as being more dorsal, but Novacek (1982) interpreted the "rhinal fissure" of Moodie (1922) as being a neocortical sulcus and not the rhinal fissure. Moodie (1922) did not annotate the orbitotemporal vessels. However, based on figures 6 and 8 (Moodie 1922), a structure ventral to the annotated rhinal fissure is likely the orbitotemporal vessels. Based on figure

5 (Moodie 1922), the annotated rhinal fissure appears to be in the same position as in our specimens.

In lateral view, the rhinal fissure is medial (behind) to the orbitotemporal vessels when present in Euarchontoglires (e.g., Silcox et al. 2010; Bertrand et al. 2016; Harrington et al. 2016) and some notoungulates (Fernández-Monescillo et al. 2019). However, this is not always the case in mammals as illustrated by *Tenrec eucaudatus* (Afrotheria; Benoit et al. 2013: fig.2) and xenarthrans (e.g., Tambusso and Fariña 2015b; Troyelli et al. 2023), in which the rhinal fissure is dorsal to the orbitotemporal vessels. It is also the case in fossils such as in some notoungulates and litopterns (Dechaseaux 1962; Dozo and Martínez 2015; Forasiepi et al. 2016), pantodonts (Muizon et al. 2015), palaeanodonts (Cabasés Bru et al. in press), basal ungulates (Orliac et al. 2012, 2023), basal cetaceans (Orliac and Thewissen 2021; Waqas et al. 2025), and to some degree in tillodonts (Bertrand et al. 2024). In fossil chiropterans, the rhinal fissure has been described as ventral to the orbitotemporal vessels in the posterior region and overlapping with the orbitotemporal vessels anteriorly (= orbitotemporal canal in Maugoust and Orliac 2021).

Based on our interpretations of the brain endocasts of *Leptictis*, we propose that the neocortex of *Leptictis* was not more developed that the paleocortex, contra Novacek (1982), and we agree with Moodie's (1922) interpretation that the rhinal fissure is located dorsal to the orbitotemporal vessels. The orbital sulcus of Moodie (1922) might be a presylvian sulcus similar to the one present in *Metacheiromys* (Cabasés Bru et al. in press). However, in *Metacheiromys*, the anterior gyrus, identified as the orbital gyrus, is much larger and is more similar in shape to the one present in their potentially closest relatives, Pholidota, than in *Leptictis*. Based on the similar position, we could propose that they may be homologous structures that would have evolved independently in different clades. The same configuration is present in two natural endocasts of *Leptictis* (Fig. 5). We note that the orbital gyrus and presylvian sulcus are also present in other mammalian clades including Xenarthra (Tambusso and Fariña 2015a; Boscaini et al. 2020a, b; Troyelli et al. 2023), Carnivora (Radinsky 1977; Lyras and Van der Geer 2003; Dubied et al. 2019), and Afrotheria (Benoit et al. 2013).

The colliculi are not visible in some specimens of *Leptictis* as Novacek (1982) observed. Indeed, the midbrain can be difficult to discern on the surface of the virtual endocasts of *Leptictis*, but it appears to be exposed just posterior to the confluence of sinuses, anterior to the vermis, and in between the two dorsal cerebellar veins oriented anterioposteriorly that connect to the transverse sinus anteriorly. Interestingly, the inferior colliculi are exposed in a natural endocast of *L. dakotensis* (Fig. 5A). Additionally, the fissure prima on the cerebrum is not visible on neither of the virtual endocasts, which was also noted by Wible and Bertrand (2024) based on the analysis of the same crania. Finally, in lateral view, the vermis is slightly more ventral than the neocortex in *L. haydeni*, but they are at the same level in *L. dakotensis*. Therefore, we agree with Novacek (1982) that there is variation of this feature within the genus *Leptictis*. However, in contrast to Novacek's (1982) hypothesis, this is unlikely related to the size of the neocortex because *L. dakotensis* (SDSM 62369) has a more expanded neocortex (13.2%) compared to *L. haydeni* (ANSP 11402; 11.3%).

Quantitative evaluation of the brain endocasts of *Leptictis*.—As noted by Novacek (1982), lateral sulci were likely present in *Leptictis*, which is not surprising based on its overall brain size (above 5 cm^3; e.g., Bauchot and Stephan 1967; Striedter 2005; Macrini et al. 2007). Based on early studies (Dechaseaux 1964; Le Gros Clark 1932), Novacek (1982) proposed that *Leptictis* had a larger neocortex in comparison to several lipotyphlans (i.e., *Solenodon*, *Erinaceus*, *Echinosorex*, and *Neurogymnurus*) and one afrosoricidan (*Tenrec*). Using data published after Novacek (1982) (i.e., Stephan et al. 1991; Boddy et al. 2012; Benoit et al. 2013), the neocortical ratio is between 11.9–26.4% for Lipotyphla, 5.7–26.2% for Afrosoricida, and 26.0–31.6% for Macroscelidea (the sister-clade to Afrosoricida). The values for *Leptictis* are 13.21% and 11.26%, which positions this genus in the low range of extant lipotyphlans and about equal to the median of afrosoricidans. In comparison to macroscelideans, *Leptictis* has a relatively smaller neocortex (Fig. 4B; SOM: table S1).

Novacek (1982) found an EQ between 0.45 and 0.70 using the Jerison (1973) equation depending on the body mass chosen for *Leptictis*. We preferred to use an average body mass to calculate the EQ because it provides a way to account for all estimates but does not give a particular weight to a specific body mass value. To calculate the EQ, Novacek (1982) proposed a body mass of 600–800 g for *Leptictis*, which is close to our average values for both specimens (743 g and 967 g). Using Jerison (1973) equation, our EQ value is 0.43 for both specimens, based on an average body mass using dental, cranial, and postcranial data. Based on the same data as for the neocortex, we find that Lipotyphla has an EQ between 0.24–1.62, Afrosoricida 0.21–0.57, and Macroscelidea 0.69–0.97. When comparing to the published data, *Leptictis* is in the middle of the range of variation of lipotyphlans and afrosoricidans but again below the range for macroscelideans (Fig. 4A; SOM: table S1). In contrast to Novacek's (1982) conclusions, this EQ value does not show that *Leptictis* was highly encephalized in comparison to these extant mammals and suggests a more complex picture. Indeed, the range for lipotyphlans and macroscelideans contains taxa with much higher EQs.

More broadly, *Leptictis* does not appear especially derived compared to early Cenozoic taxa. Since Novacek's (1982) work, numerous brain endocasts of Mesozoic (Rowe et al. 2011; Csiki-Sava et al. 2018; Bertrand et al. 2026 for a review) and early Cenozoic (e.g., Bertrand et al. 2020, 2022; Dozo et al. 2023) taxa have been published. In terms of the relative size of the neocortex, early Oligocene *Leptictis* falls within the range of Paleocene (10.3–19.9%) and Eocene (7.8–43.8%) taxa. The phylogenetic encephalization quotient (PEQ), a phylogenetically corrected version of the EQ that

we use here, was measured for a large number of Mesozoic and early Cenozoic mammals in Bertrand et al. (2022). In the latter work, *Leptictis* was placed at the base of Placentalia and not close to any of the placental crown groups because of its uncertain phylogenetic position: within Afrotheria (O'Leary et al. 2013) or outside of Placentalia (Halliday et al. 2017; Wible et al. 2009). Even though the specimen that was included, *L. dakotensis* (SDSM 62369), is from the early Oligocene, it has a lower PEQ (0.30) than many Eocene taxa, which range from 0.08–0.83. However, it has a higher PEQ than any Paleocene (0.04–0.23) and most Mesozoic taxa (0.11–0.31, except *Vintana*; Kirk et al. 2014).

Novacek (1982) concluded that *Leptictis* had intermediate-sized olfactory bulbs when compared to a sample of lipotyphlans, macroscelideans, and plesiadapiforms. Using the same sources as for the neocortical ratio and EQ, we find that Lipotyphla has an olfactory bulb ratio between 3.0–10.3%, Afrosoricida 2.0–14.7%, and Macroscelidea 5.2–9.3%. *Leptictis* falls in the mid-range of lipotyphlans and afrosoricidans, and in the upper range of variation for macroscelideans (Fig. 4C). To deduce whether or not specialization occurred in the lineage leading to *Leptictis*, we would need to know which clades are their closest relatives, which is still debated (e.g., O'Leary et al. 2013; Velazco et al. 2022; Wible et al. 2007). The olfactory bulb ratio of *Leptictis* is also in the range of Mesozoic (5.9–14.5%) and early Cenozoic mammals (0.9–16.8%). The ancestral condition for mammals for the size of the olfactory bulbs is difficult to determine because of the wide range observed in Mesozoic mammals. Regardless, we agree with Novacek (1982) that the olfactory bulbs of *Leptictis* (8.4% and 9.3%) are intermediate in size in comparison to other mammals.

Phylogenetic signal in endocranial structures.—A potential close relationship between *Leptictis* and *Eoryctes* has been proposed based on basicranial anatomy by Wible and Bertrand (2024). The brain endocranial anatomy of *Eoryctes* has been described based on a latex endocast (Thewissen and Gingerich 1989). Both taxa have an overall very similar brain morphology that is likely plesiomorphic, including the presence of a relatively small neocortex (no quantitative data for *Eoryctes*). Regarding the rhinal fissure of *Eoryctes*, Thewissen and Gingerich (1989) identified it at the level of the orbitotemporal vessels as in *Leptictis* (Novacek 1982). Similar to *Leptictis*, we argue that this is a misidentification and that the rhinal fissure is located more dorsally, and that their "marginal sulcus" is likely the rhinal fissure. The brain of *Eoryctes* was estimated to be about 1 cm^3 (Thewissen and Gingerich 1989), which is likely too small to be gyrencephalic (>5 cm^3; Macrini et al. 2007). *Eoryctes* displays a broad exposure of the inferior colliculi (Thewissen and Gingerich 1989) but based on only one specimen. In *Leptictis*, it appears that the exposure of the colliculi is variable with some specimens only showing a small patch of midbrain (SDSM 62369, ANSP 11402, AMNH F: AM 96730), while at least one specimen (AMNH F: AM 87458) displays exposed inferior colliculi similar to *Eoryctes*. However, the exposure appears larger in *Eoryctes* compared to *Leptictis* sp. AMNH F: AM 87458. The broad exposure of the inferior colliculi could represent a sensory specialization (see Edinger 1964). However, Bertrand et al. (2026: fig. 5a) showed that for a sample of Cretaceous, Paleocene, and Eocene mammals, species with absolutely smaller endocranial volumes may be significantly more likely to have exposed colliculi. The challenge will be to reconcile the functional importance of exposed colliculi and (i) its degree of expansion, (ii) the fact that they are more likely to be seen in small brains, and (iii) that intraspecific variation is likely to be present. Indeed, intraspecific variation has been shown to be present in other mammals including rodents and plesiadapiforms (Silcox et al. 2010; Bertrand and Silcox 2016).

The vascular system of *Leptictis* was compared with *Eoryctes* in Wible and Bertrand (2024). Some noted similarities were the presence of the condyloid canals and orbitotemporal vessels, a large size for the sulcus of the sigmoid sinus and a frontal diploic vein (also noted by Thewissen and Gingerich 1989). All of these features likely do not represent a phylogenetic signal, particularly the large size of the sulcus for the sigmoid sinus. For instance, among early-diverging placental mammals, the Eocene taxa *Trogosus* (Bertrand et al. 2024) and *Metacheiromys* (Cabasés Bru et al. in press) also display relatively large sigmoid sinuses, indicating that it is probably a plesiomorphic feature. One interesting difference noted by Wible and Bertrand (2024) is that the internal carotid artery, stapedial artery, and facial nerve are within canals in *Eoryctes*, while in *Leptictis*, the passageways for the facial nerve and the arteries are within canals when close to the brain cavity, but in grooves on the tympanic surface of the petrosal. There is also a ramus inferior branch of the internal carotid artery in *Eoryctes* but it is absent in *Leptictis* (Wible and Bertrand 2024). Overall, the endocranial anatomy and vascular system do not appear to provide concrete evidence of shared derived characters that would denote close phylogenetic relationship between *Leptictis* and *Eoryctes*. This is not surprising as these taxa have been difficult to position in the tree of mammals.

Neurosensory ecology.—Based on postcranial data, *Leptictis* may have been cursorial to possibly saltatorial and may have had digging adaptations (Rose 2006). The neocortex is relatively small, the olfactory bulbs are of intermediate size, and the petrosal lobules (which relate to maintenance of the control of eye and head movements; Rambold et al. 2002) are relatively small. This combination of features could suggest a higher reliance on olfaction than other senses such as vision. However, the presence of a presylvian sulcus and the orbital gyrus could be linked to specific functions associated with assessing sensory objects such as food items and especially flavor, appearance, and texture (Rolls 2005; Price 2007). Ultimately, without a phylogenetic context, it is difficult to reconstruct the neurosensory ecology of *Leptictis*. Ideally, we would need to compare the size of

these brain regions in *Leptictis* with more basal and closely related taxa to understand potential shifts in senses. One particular ecological adaptation, fossoriality, may lead to decrease in different brain components including the petrosal lobules (Bertrand et al. 2018; Cabasés Bru et al. in press). As *Leptictis* has been found in burrows (Sundell 1997), it is possible that its neurosensory system reflects adaptations to some degree of fossoriality. What is clear is that the brain endocast of *Leptictis* does not show any extreme sensory specializations in contrast to *Eoryctes,* which potentially has a very broad exposure of the inferior colliculi and the presence of relatively large olfactory bulbs (~16%) as noted by Thewissen and Gingerich (1989).

Conclusions

In this report, we use CT data to generate the first digital brain endocasts of the well-known but phylogenetically controversial early Oligocene placental mammal (or close relative), *Leptictis.* This provides new information on the endocranial brain anatomy of *L. dakotensis* and the first description of the brain endocast of *L. haydeni*. Both specimens present very similar anatomies. Some variation is observed in the vascular system but is of uncertain value given the poorer preservation in the specimen of *L. dakotensis.* One genuine difference is the separation of the condyloid canal into two canals when exiting the endocranial cavity in *L. haydeni*, while *L. dakotensis* displays only one canal. Another anatomical feature previously not identified in earlier studies of *Leptictis* endocranial anatomy by Moodie (1922), Novacek (1982), and Wible and Bertrand (2024) is the dorsal cerebellar vein, which we show is present in both specimens. For the first time, we also illustrate the ventral aspect of the endocranial anatomy illustrating the exit of cranial nerves and associated vessels. We re-interpret the position of the rhinal fissure as being more dorsal than identified by Novacek (1982) and agree with Moodie (1922) interpretation. This finding suggests that *Leptictis* did not have a more expanded neocortex in comparison to extant Lipotyphla and Afroinsectivora (i.e., Afrosoricida and Macroscelidea). We support the potential presence of lateral sulci in *L. dakotensis.*

In contrast to previous work, the EQ shows that *Leptictis* was not specifically encephalized compared to Lipotyphla and Afrosoricida and lower than Macroscelidea. The early Oligocene *Leptictis* is not specifically derived and is in the range of variation for neocortical size of Paleocene and Eocene taxa. However, it has a PEQ higher than Paleocene and most Mesozoic taxa but in the range of Eocene species. The olfactory bulbs are intermediate in size and fall in the range of extant Lipotyphla, Afrosoricida, Macroscelidea, Mesozoic, and early Cenozoic taxa. The midbrain is exposed in both specimens of *Leptictis,* but in contrast to previous work, we observe variation in the presence of the inferior colliculi. It remains unclear if this observation might represent sensory specialization.

We were unable to find endocranial features that represent a close phylogenetic relationship between *Leptictis* and *Eoryctes*. Indeed, the observed morphological similarities are likely to be plesiomorphic features. We note that the rhinal fissure has also likely been misidentified in *Eoryctes* and that the separation between the neocortex and the paleocortex is more dorsal as found in *Leptictis.* In terms of neurosensory ecology, it is possible that the relatively small neocortex and petrosal lobules might be associated with fossorial adaptations in *Leptictis.* The CT scanning and generation of brain endocasts of other taxa such as *Megalepticis*, *Blacktops*, and *Stenoleptictis* that preserve complete braincases (Korth 2022; Meehan and Martin 2010, 2012) would greatly improve our understanding of potential sensory evolutionary shifts within Leptictidae.

Authors' contributions

OCB, CCVG, and SLB conceived and designed the study, based on an earlier study of early placental mammal brains developed by OCB, JRW, and SLB. Supervision of CCVG was performed by OCB and SLB. OCB, and SLB acquired the CT data of the fossil specimens. CCVG and OCB did the segmentations. CCVG drafted the manuscript, tables, and some of the figures. LK gathered the quantitative data on extant taxa and made the boxplots. These files were revised by OCB, JRW, and SLB. Analyses and interpretations were performed by OCB, CCVG, JRW, and LK, and critically reviewed by SLB. All authors revised the manuscript and provided final approval before submission.

Data archiving statement

Data to generate the boxplots are available in SOM: table S1.The 3D models of the virtual endocasts are available in Morphosource: https://www.morphosource.org/projects/000815256?locale=en

Acknowledgements

This project started as the Master's project of Carl C. Van Gent at the University of Edinburgh in the UK. We thank Morgan Mill Chase for assistance in scanning the specimens at the Microscopy and Imagery Facility (MIF) at the AMNH. For access to the specimens, we thank Michael J. Novacek and Suzann Goldberg (both AMNH); for permission to study the CT scans, we thank Edward Daeschler (Academy of Natural Sciences of Drexel University, Philadelphia, USA); Bruce A. Schumacher (US Forest Service, Lakewood, Colorado), and Darrin C. Pagnac (South Dakota School of Mines, Rapid City, USA). This work was supported by Marie Skłodowska-Curie Actions: Individual Fellowship, H2020-MSCA-IF-2018-2020, no. 792611 (OCB); Beatriu de Pinós Programme funded by the Direcció General de Recerca de la Generalitat de Catalunya and managed by AGAUR, expedient number: 2021 BP 00042 (OCB); Ramón y Cajal, Ayuda RYC2023-042630-I financiada por MICIU/AEI/10.13039/501100011033 y por el FSE+ (OCB); European Research Council (ERC) Starting Grant 756226 under the European Union's Horizon 2020 Research and Innovation Programme, 10.13039/100010663, H2020 European Research Council (SLB); Leverhulme Trust, Philip Leverhulme Prize (SLB); NSF DEB 1654952 (SLB); Swedish Research Council Grant 2021-02973 (SLB);

NSF DEB 1654949 (JRW); the R.K. Mellon North American Mammal Research Institute (JRW); OCB is a member of the Project PID2024-156593NB-I00 funded by the MICIU/AEI /10.13039/501100011033 y por FEDER, UE; OCB was also supported by the CERCA Programme/ Generalitat de Catalunya. We would like to thank Maëva Orliac (Institut des Sciences de l'Evolution de Montpellier, France) and Sebastián Tambusso (Instituto de Investigaciones Biológicas Clemente Estable, Montevideo, Uruguay) for their reviews that improved the quality of this manuscript. There are no conflicts of interest.

Editor: Eli Amson

References

Asher, R.J. and Helgen, K.M. 2010. Nomenclature and placental mammal phylogeny. *BMC Evolutionary Biology* 10: 102.

Asher, R.J., Novacek, M.J., and Geisler, J.H. 2003. Relationships of endemic African mammals and their fossil relatives based on morphological and molecular evidence. *Journal of Mammalian Evolution* 10: 131–194.

Bauchot, R. and Stephan, H. 1967. Encéphales et moulages endocraniens de quelques insectivores et primates actuels. *In: Problèmes actuels de paléontologie (évolution des vertébrés): colloques Internationaux du centre national de la recherche scientifique* 163: 575–587. Editions du centre national de la recherche scientifique, Paris.

Benoit, J., Crumpton, N., Mérigeaud, S., and Tabuce, R. 2013. A memory already like an elephant's? The advanced brain morphology of the last common ancestor of Afrotheria (Mammalia). *Brain, Behavior and Evolution* 81: 154–169.

Bertrand, O.C. and Silcox, M.T. 2016. First virtual endocasts of a fossil rodent: *Ischyromys typus* (Ischyromyidae, Oligocene) and brain evolution in rodents. *Journal of Vertebrate Paleontology* 36: 1–19.

Bertrand, O.C., Amador-Mughal, F., and Silcox, M.T. 2016. Virtual endocasts of Eocene *Paramys* (Paramyinae): oldest endocranial record for Rodentia and early brain evolution in Euarchontoglires. *Proceedings of the Royal Society B: Biological Sciences* 283: 1–8.

Bertrand, O.C., Amador-Mughal, F., and Silcox, M.T. 2017. Virtual endocast of the early Oligocene *Cedromus wilsoni* (Cedromurinae) and brain evolution in squirrels. *Journal of Anatomy* 230: 128–151.

Bertrand, O.C., Amador-Mughal, F., Lang, M.M., and Silcox, M.T. 2018. Virtual endocasts of fossil Sciuroidea: brain size reduction in the evolution of fossoriality. *Palaeontology* 61: 919–948.

Bertrand, O.C., Amador-Mughal, F., Lang, M.M., and Silcox, M.T. 2019. New virtual endocasts of Eocene Ischyromyidae and their relevance in evaluating neurological changes occurring through time in Rodentia. *Journal of Mammalian Evolution* 26: 345–371.

Bertrand, O.C., Jiménez Lao, M., Shelley, S.L., Wible, J.R., Williamson, T.E., Meng, J., and Brusatte, S.L. 2024. The virtual brain endocast of *Trogosus* (Mammalia, Tillodontia) and its relevance in understanding the extinction of archaic placental mammals. *Journal of Anatomy* 244: 1–21.

Bertrand, O.C., Michaud, M., and Kirk, E.C. 2026. How the neurosensory system provides clues for the adaptive radiation of mammals. *In*: J.H. Kaas and S. Herculano-Houzel (eds.), *Evolution of Nervous Systems in Mammals. Evolution of Nervous Systems*, 57–85. Academic Press, Oxford.

Bertrand, O.C., Shelley, S.L., Wible, J.R., Williamson, T.E., Holbrook, L.T., Chester, S.G.B., Butler, I.B., and Brusatte, S.L. 2020. Virtual endocranial and inner ear endocasts of the Paleocene 'condylarth' *Chriacus*: New insight into the neurosensory system and evolution of early placental mammals. *Journal of Anatomy* 236: 21–49.

Bertrand, O.C., Shelley, S.L., Williamson, T.E., Wible, J.R., Chester, S.G.B., Flynn, J.J., Holbrook, L.T., Lyson, T.R., Meng, J., Miller, I.M., Püschel, H.P., Smith, T., Spaulding, M., Tseng, Z.J., and Brusatte, S.L. 2022. Brawn before brains in placental mammals after the end-Cretaceous extinction. *Science* 376: 80–85.

Boddy, A.M., Mcgowen, M.R., Sherwood, C.C., Grossman, L.I., Goodman, M., and Wildman, D.E. 2012. Comparative analysis of encephalization in mammals reveals relaxed constraints on anthropoid primate and cetacean brain scaling. *Journal of Evolutionary Biology* 25: 981–994.

Boscaini, A., Iurino, D.A., Mamani Quispe, B., Andrade Flores, R., Sardella, R., Pujos, F., and Gaudin, T.J. 2020a. Cranial anatomy and paleoneurology of the extinct sloth *Catonyx tarijensis* (Xenarthra, Mylodontidae) from the Late Pleistocene of Oruro, southwestern Bolivia. *Frontiers in Ecology and Evolution* 8: 1–16.

Boscaini, A., Iurino, D.A., Sardella, R., Tirao, G., Gaudin, T.J., and Pujos, F. 2020b. Digital cranial endocasts of the extinct sloth *Glossotherium robustum* (Xenarthra, Mylodontidae) from the Late Pleistocene of Argentina: Description and comparison with the extant sloths. *Journal of Mammalian Evolution* 27: 55–71.

Burger, J.R., George, M.A., Jr., Leadbetter, C., and Shaikh, F. 2019. The allometry of brain size in mammals. *Journal of Mammalogy* 100: 276–283.

Cabasés Bru, E., Moya-Costa, R., Wible, J.R., Brusatte, S.L., and Bertrand, O.C. (in press). Virtual brain endocasts of the palaeanodont *Metacheiromys marshi* and the neurosensory evolution of early Pholidotamorpha. *Journal of Anatomy* [available online, https://doi.org/10.1111/joa.70142].

Campione, N.E. and Evans, D.C. 2012. A universal scaling relationship between body mass and proximal limb bone dimensions in quadrupedal terrestrial tetrapods. *BMC Biology* 10: 60.

Csiki-Sava, Z., Vremir, M., Meng, J., Brusatte, S.L., and Norell, M.A. 2018. Dome-headed, small-brained island mammal from the Late Cretaceous of Romania. *Proceedings of the National Academy of Sciences* 115: 4857–4862.

Damuth, J. 1990. Problems in estimating body masses of archaic ungulates using dental measurements. *In*: J. Damuth, B.J. MacFadden (eds.), *Body Size in Mammalian Paleobiology: Estimation and Biological Implications*, 229–253. Cambridge University Press, Cambridge.

Dechaseaux, C. 1962. Encefalos de notoungulados y de desdentados xenartros fosiles. *Ameghiniana* 2: 193–209.

Dechaseaux, C. 1964. L'encéphale de *Neurogymnurus cayluxi* Insectivore des Phosphorites de Quercy. *Annales de Paléontologie* 50: 83–100.

Dozo, M.T. and Martínez, G. 2015. First digital cranial endocasts of late Oligocene Notohippidae (Notoungulata): Implications for endemic South American ungulates brain evolution. *Journal of Mammalian Evolution* 23: 1–16.

Dozo, M.T., Paulina-Carabajal, A., Macrini, T.E., and Walsh, S. 2023. *Paleoneurology of amniotes: New directions in the study of fossil endocasts*. 840 pp. Springer, Cham.

Dubied, M., Solé, F., Mennecart, B., and Hautier, L. 2019. The cranium of *Proviverra typica* (Mammalia, Hyaenodonta) and its impact on hyaenodont phylogeny and endocranial evolution. *Palaeontology* 62: 983–1001.

Edinger, T. 1964. Midbrain exposure and overlap in mammals. *American Zoologist* 4: 5–19.

Eisenberg, J.F. 1981. *The mammalian radiations: An analysis of trends in evolution, adaptation, and behavior*. 610 pp. University of Chicago Press, Chicago.

Engelman, R.K. 2022. Occipital condyle width (OCW) is a highly accurate predictor of body mass in therian mammals. *BMC Biology* 20: 1–44.

Fernández-Monescillo, M., Antoine, P.-O., Pujos, F., Gomes Rodrigues, H., Mamani Quispe, B., and Orliac, M. 2019. Virtual endocast morphology of Mesotheriidae (Mammalia, Notoungulata, Typotheria): New insights and implications on notoungulate encephalization and brain evolution. *Journal of Mammalian Evolution* 26: 85–100.

Forasiepi, A.M., MacPhee, R.D.E., Del Pino, S.H., Schmidt, G.I., Amson, E., and Grohé, C. 2016. Exceptional skull of *Huayqueriana* (Mammalia, Litopterna, Macraucheniidae) from the late Miocene of Argentina: Anatomy, systematics, and paleobiological implications. *Bulletin of the American Museum of Natural History* 2016: 1–76.

Gidley, J.W. 1915. An extinct marsupial from the Fort Union with notes on the Myrmecobidae and other families of this group. *Proceedings of the United States National Museum* 48: 395–402.

Gingerich, P.D. and Smith, T. 2006. Paleocene–Eocene land mammals from three new latest Clarkforkian and earliest Wasatchian wash sites at Polecat Bench in the northern Bighorn Basin, Wyoming. *Contributions from the Museum of Paleontology, University of Michigan* 31: 245–303.

Gunnell, G.F. and Bloch, J.I. 2008. Insectivorous mammals summary. *In*: C.M. Janis, G.F. Gunnell, and M.D. Uhen (eds.), *Evolution of Tertiary Mammals of North America, vol 2*, 49–62. Cambridge University Press, Cambridge.

Gunnell, G.F., Bown, T.M., and Bloch, J.I. 2008. Leptictida. *In*: C.M. Janis, G.F. Gunnell, and M.D. Uhen (eds.), *Evolution of Tertiary Mammals of North America, Vol 2*, 82–88. Cambridge University Press, Cambridge.

Gunnell, G.F., Zonneveld, J.-P., and Bartels, W.S. 2016. Stratigraphy, mammalian paleontology, paleoecology, and age correlation of the Wasatch Formation, Fossil Butte National Monument, Wyoming. *Journal of Paleontology* 90: 981–1011.

Halliday, T.J.D., Upchurch, P., and Goswami, A. 2017. Resolving the relationships of Paleocene placental mammals. *Biological Reviews* 92: 521–550.

Harrington, A.R., Silcox, M.T., Yapuncich, G.S., Boyer, D.M., and Bloch, J.I. 2016. First virtual endocasts of adapiform primates. *Journal of Human Evolution* 99: 52–78.

Herculano-Houzel, S. 2012. The remarkable, yet not extraordinary, human brain as a scaled-up primate brain and its associated cost. *Proceedings of the National Academy of Sciences* 109: 10661–10668.

Hooker, J.J. 2013. Origin and evolution of the Pseudorhyncocyonidae, a European Paleogene family of insectivorous placental mammals. *Palaeontology* 56: 807–835.

Janis, C.M., Gunnell, G.F., and Uhen, M.D. 2008. *Evolution of Tertiary Mammals of North America: Volume 2, Small Mammals, Xenarthrans, and Marine Mammals*. 804 pp. Cambridge University Press, Cambridge.

Jerison, H.J. 1973. *Evolution of the Brain and Intelligence*. 498 pp. Academic Press, New York.

Jerison, H.J. 2012. Digitized fossil brains: neocorticalization. *Biolinguistics* 6: 383–392.

Kellner, A.W.A. and McKenna, M.C. 1996. A leptictid mammal from the Hsanda Gol Formation (Oligocene), Central Mongolia, with comments on some Palaeoryctidae. *American Museum Novitates* 3168: 1–13.

Kirk, E.C., Hoffmann, S., Kemp, A.D., Krause, D.W., and O'Connor, P.M. 2014. Sensory anatomy and sensory ecology of *Vintana sertichi* (Mammalia, Gondwanatheria) from the Late Cretaceous of Madagascar. *Journal of Vertebrate Paleontology* 34: 203–222.

Korth, W.W. 2022. New material of leptictids (Mammalia: Leptictida) from the late Eocene (Duchesnean–Chadronian) of southwestern Montana. *Annals of Carnegie Museum* 87: 309–326.

Lang, M.M., Bertrand, O.C., San Martin-Flores, G., Law, C.J., Abdul-Sater, J., Spakowski, S., and Silcox, M.T. 2022. Scaling patterns of cerebellar petrosal lobules in Euarchontoglires: impacts of ecology and phylogeny. *The Anatomical Record* 305: 3472–3503.

Le Gros Clark, W.E. 1932. The brain of the Insectivora. *Proceedings of the Zoological Society of London* 102: 975–1013.

Legendre, S. 1989. Les communautés de mammifères du Paléogène (Eocène supérieur et Oligocène) d'Europe occidentale: structures, milieux et évolution. *Geowissenschaftliche Abhandlungen, Reihe A, Geologie und Paläontologie* 16: 1–110.

Leidy, J. 1868. Notice of some remains of extinct Insectivora from Dakota. *Proceedings of the Academy of Natural Sciences of Philadelphia*: 315–316.

Long, A., Bloch, J.I., and Silcox, M.T. 2015. Quantification of neocortical ratios in stem primates. *American Journal of Physical Anthropology* 157: 363–373.

Lyras, G.A. and Van der Geer, A.A.E. 2003. External brain anatomy in relation to the phylogeny of Caninae (Carnivora: Canidae). *Zoological Journal of the Linnean Society* 138: 505–522.

Macrini, T.E., Rougier, G.W., and Rowe, T. 2007. Description of a cranial endocast from the fossil mammal *Vincelestes neuquenianus* (Theriiformes) and its relevance to the evolution of endocranial characters in therians. *The Anatomical Record* 290: 875–892.

Martin, R.D. 1990. Evolution of the primate central nervous system. *In*: R.D. Martin (ed.), *Primate Origins and Evolution. A Phylogenetic Reconstruction*, 357–426. Princeton University Press, Princeton.

Matthew, W. 1929. Preoccupied names. *Journal of Mammalogy* 10: 1–7.

Matthew, W.D. 1899. A provisional classification of the fresh-water Tertiary of the West. *Bulletin of the American Museum of Natural History* 12: 19–75.

Matthew, W.D. and Granger, W. 1921. New genera of Paleocene mammals. *American Museum Novitates* 13: 1–7.

Maugoust, J. and Orliac, M.J. 2021. Endocranial cast anatomy of the extinct hipposiderid bats *Palaeophyllophora* and *Hipposideros* (*Pseudorhinolophus*) (Mammalia: Chiroptera). *Journal of Mammalian Evolution* 28: 679–706.

McKenna, M.C. and Bell, S.K. 1997. *Classification of Mammals: Above the Species Level*. 640 pp. Columbia University Press, New York.

Meehan, T. and Martin, L.D. 2010. New leptictids (Mammalia: lnsectivora) from the early Oligocene of Nebraska, USA. *Neues Jahrbuch für Geologie und Palaontologie, Abhandlungen* 256: 99–107.

Meehan, T. and Martin, L.D. 2012. New large leptictid insectivore from the late Paleogene of South Dakota, USA. *Acta Palaeontologica Polonica* 57: 509–518.

Moodie, R.L. 1922. On the endocranial anatomy of some Oligocene and Pleistocene mammals. *The Journal of Comparative Neurology* 34: 343–379.

Morlo, M., Schaal, S., Mayr, G., and Seiffert, C. 2004. An annotated taxonomic list of the middle Eocene (MP 11) Vertebrata of Messel. *Courier Forschungsinstitut Senckenberg* 252: 95–108.

Muizon, C. de, Billet, G., Argot, C., Ladevèze, S., and Goussard, F. 2015. *Alcidedorbignya inopinata*, a basal pantodont (Placentalia, Mammalia) from the early Palaeocene of Bolivia: Anatomy, phylogeny and palaeobiology. *Geodiversitas* 37: 397–634.

Murphy, W.J., Foley, N.M., Bredemeyer, K.R., Gatesy, J., and Springer, M.S. 2021. Phylogenomics and the genetic architecture of the placental mammal radiation. *Annual Review of Animal Biosciences* 9: 29–53.

Novacek, M.J. 1976. Early Tertiary vertebrate faunas, Vieja Group, Trans-Pecos Texas: Insectivora. *The Pierce Sellards Series, Texas Memorial Museum* 23: 1–17.

Novacek, M.J. 1977. A review of Paleocene and Eocene Leptictidae (Eutheria: Mammalia) from North America. *PaleoBios* 24: 1–42.

Novacek, M.J. 1982. The brain of *Leptictis dakotensis*, an Oligocene leptictid (Eutheria: Mammalia) from North America. *Journal of Paleontology* 56: 1177–1186.

Novacek, M.J. 1986. The skull of leptictid insectivorans and the higher-level classification of eutherian mammals. *Bulletin of the American Museum of Natural History* 183: 1–112.

O'Leary, M.A., Bloch, J.I., Flynn, J.J., Gaudin, T.J., Giallombardo, A., Giannini, N.P., Goldberg, S.L., Kraatz, B.P., Luo, Z.X., Meng, J., Ni, X., Novacek, M.J., Perini, F.A., Randall, Z.S., Rougier, G.W., Sargis, E.J., Silcox, M.T., Simmons, N.B., Spaulding, M., Velazco, P.M., Weksler, M., Wible, J.R., and Cirranello, A.L. 2013. The placental mammal ancestor and the post-K-Pg radiation of placentals. *Science* 339: 662–667.

Orliac, M.J., Argot, C., and Gilissen, E. 2012. Digital cranial endocast of *Hyopsodus* (Mammalia, "Condylarthra"): A case of Paleogene terrestrial echolocation? *PloS one* 7: e30000.

Orliac, M.J., Maugoust, J., Balcarcel, A., and Gilissen, E. 2023. Paleoneurology of Artiodactyla, an overview of the evolution of the artiodactyl brain. *In*: M.T. Dozo, A. Paulina-Carabajal, T.E. Macrini, and S. Walsh (eds.), *Paleoneurology of Amniotes: New Directions in the Study of Fossil Endocasts*, 507–555. Springer, Cham.

Orliac, M.J. and Thewissen, J.G.M. 2021. The endocranial cast of *Indohyus* (Artiodactyla, Raoellidae): The origin of the cetacean brain. *Journal of Mammalian Evolution* 28: 831–843.

Price, J.L. 2007. Definition of the orbital cortex in relation to specific connections with limbic and visceral structures and other cortical regions. *Annals of the New York Academy of Sciences* 1121: 54–71.

R Core Team 2019. *R: A Language and Environment for Statistical Computing*. R Foundation for Statistical Computing, Vienna.

Radinsky, L. 1977. Brains of early carnivores. *Paleobiology* 3: 333–349.

Rambold, H., Churchland, A., Selig, Y., Jasmin, L., and Lisberger, S.G. 2002. Partial ablations of the flocculus and ventral paraflocculus in monkeys cause linked deficits in smooth pursuit eye movements and adaptive modification of the VOR. *Journal of Neurophysiology* 87: 912–924.

Rolls, E.T. 2005. Taste, olfactory, and food texture processing in the brain, and the control of food intake. *Physiology & Behavior* 85: 45–56.

Rose, K.D. 1999. Postcranial skeleton of Eocene Leptictidae (Mammalia), and its implications for behavior and relationships. *Journal of Vertebrate Paleontology* 19: 355–372.

Rose, K.D. 2006. The postcranial skeleton of early Oligocene *Leptictis* Mammalia: Leptictida), with a preliminary comparison to *Leptictidium* from the middle Eocene of Messel. *Palaeontographica, Abteilung A* 278: 37–56.

Rose, K.D. 2012. The importance of Messel for interpreting Eocene Holarctic mammalian faunas. *Palaeobiodiversity and Palaeoenvironments* 92: 631–647.

Rowe, T.B., Macrini, T.E., and Luo, Z.X. 2011. Fossil evidence on origin of the mammalian brain. *Science* 332: 955–957.

Seiffert, E.R. 2007. A new estimate of afrotherian phylogeny based on simultaneous analysis of genomic, morphological, and fossil evidence. *BMC Evolutionary Biology* 7: 1–13.

Silcox, M.T., Benham, A.E., and Bloch, J.I. 2010. Endocasts of *Microsyops* (Microsyopidae, Primates) and the evolution of the brain in primitive primates. *Journal of Human Evolution* 58: 505–521.

Smith, F.A., Lyons, S.K., Ernest, S.K.M., Jones, K.E., Kaufman, D.M., Dayan, T., Marquet, P.A., Brown, J.H., and Haskell, J.P. 2003. Body mass of late Miocene Quaternary mammals. *Ecology* 84: 3403–3403.

Stephan, H., Baron, G., and Frahm, H.D. 1991. *Insectivora: With a Stereotaxic Atlas of the Hedgehog Brain*. 573 pp. Springer-Verlag, New York.

Stephan, H., Frahm, H., and Baron, G. 1981. New and revised data on volumes of brain structures in insectivores and primates. *Folia Primatologica* 35: 1–29.

Striedter, G.F. 2005. *Principles of Brain Evolution*. 436 pp. Sinauer Associates, Sunderland.

Sundell, C. 1997. Orellan burrows and associated fauna from Converse County, WY. *Journal of Vertebrate Paleontology, Abstract Supplement* 17: 80A.

Tambusso, P.S. and Fariña, R.A. 2015a. Digital cranial endocast of *Pseudoplohophorus absolutus* (Xenarthra, Cingulata) and its systematic and evolutionary implications. *Journal of Vertebrate Paleontology* 35: e967853.

Tambusso, P.S. and Fariña, R.A. 2015b. Digital endocranial cast of *Pampatherium humboldtii* (Xenarthra, Cingulata) from the Late Pleistocene of Uruguay. *Swiss Journal of Palaeontology* 134: 109–116.

Thewissen, J.G.M. and Gingerich, P.D. 1989. Skull and endocranial cast of *Eoryctes melanus*, a new palaeoryctid (Mammalia: Insectivora) from the early Eocene of western North America. *Journal of Vertebrate Paleontology* 9: 459–470.

Tong, Y. and Wang, J. 2006. Fossil mammals from the early Eocene Wutu Formation of Shandong Province. *Palaeontologia Sinica, new series C* 28: 1–195.

Troyelli, A., Cassini, G.H., Tirao, G., Boscaini, A., and Fernicola, J.C. 2023. Endocranial cast anatomy of the early Miocene glyptodont *Propalaehoplophorus australis* (Mammalia, Xenarthra, Cingulata) and its evolutionary implications. *Journal of Mammalian Evolution* 30: 907–922.

Van Valen, L. 1965. Treeshrews, primates, and fossils. *Evolution* 19: 137–151.

Van Valen, L.M. 1967. New Paleocene insectivores and insectivore classification. *Bulletin of the American Museum of Natural History* 135: 219–284.

Vandenberghe, N., Hilgen, F.J., Speijer, R.P., Ogg, J.G., Gradstein, F.M., Hammer, O., Hollis, C.J., and Hooker, J.J. 2012. The Paleogene Period. *In*: F.M. Gradstein, J.G. Ogg, M.D. Schmitz, G.M. Ogg (eds.), *The Geologic Time Scale*, 855–921. Elsevier, Boston.

Velazco, P.M., Buczek, A.J., Hoffman, E., Hoffman, D.K., O'Leary, M.A., and Novacek, M.J. 2022. Combined data analysis of fossil and living mammals: A Paleogene sister taxon of Placentalia and the antiquity of Marsupialia. *Cladistics* 38: 359–373.

Velazco, P.M. and Novacek, M.J. 2016. Systematics of the genus *Palaeictops* Matthew, 1899 (Mammalia: Leptictidae), with the description of two new species from the middle Eocene of Utah and Wyoming. *American Museum Novitates* 2016: 1–42.

Vincent, F., Souron, A., Casanovas-Vilar, I., Gamarra, J., and Bertrand, O.C. 2025. The brain endocast of the Canary Islands giant rats (*Canariomys*, Muridae, Rodentia): Paleobiological and evolutionary implications. *Journal of Mammalian Evolution* 32: 1–28.

Wahlert, J.H. 2004. The skull and dentition of *Eumys elegans* from the Oligocene of North Dakota. *Bulletin of Carnegie Museum of Natural History* 36: 335–348.

Waqas, M., Smith, T., Rana, R., and Orliac, M.J. 2025. The endocranial cast of *Khirtharia* (Artiodactyla, Raoellidae) provides new insights into the earliest evolution of the cetacean brain. *Brain Behavior and Evolution* 100: 80–92.

Wible, J.R. 1984. *The Ontogeny and Phylogeny of the Mammalian Cranial Arterial Pattern.* 805 pp. Ph.D. Thesis, Duke University, Durham.

Wible, J.R. 1987. The eutherian stapedial artery: character analysis and implications for superordinal relationships. *Zoological Journal of the Linnean Society* 91: 107–135.

Wible, J.R. and Bertrand, O.C. 2024. Basicranial anatomy of *Leptictis haydeni* Leidy, 1868 (Mammalia, Eutheria, Leptictidae). *Annals of Carnegie Museum* 90: 1–36.

Wible, J.R. and Rougier, G.W. 2000. Cranial anatomy of *Kryptobaatar dashzevegi* (Mammalia, Multituberculata), and its bearing on the evolution of mammalian characters. *Bulletin of the American Museum of Natural History* 247: 1–120.

Wible, J.R., Rougier, G.W., Novacek, M.J., and Asher, R.J. 2007. Cretaceous eutherians and Laurasian origin for placental mammals near the K/T boundary. *Nature* 447: 1003–1006.

Wible, J.R., Rougier, G.W., Novacek, M.J., and Asher, R.J. 2009. The eutherian mammal *Maelestes gobiensis* from the Late Cretaceous of Mongolia and the phylogeny of Cretaceous Eutheria. *Bulletin of the American Museum of Natural History* 327: 1–123.

Wickham, H. 2016. *ggplot2: Elegant Graphics for Data Analysis*. 260 pp. Springer-Verlag, New York.